Retinal HDR images: Intraocular glare and object size

John J. McCann
Alessandro Rizzi

Abstract — Starting from measured scene luminances, the retinal images of high-dynamic-range (HDR) test targets were calculated. These test displays contain 40 gray squares with a 50% average surround. In order to approximate a natural scene, the surround area was made up of half-white and half-black squares of different sizes. In this display, the spatial-frequency distribution approximates a $1/f$ function of energy *vs.* spatial frequency. Images with 2.7 and 5.4 optical density ranges were compared. Although the target luminances are very different, after computing the retinal image according to the CIE scatter glare formula, it was found that the retinal ranges are very similar. Intraocular glare strongly restricts the range of the retinal image. Furthermore, uniform, equiluminant target patches are spatially transformed to different gradients with unequal retinal luminances. The usable dynamic range of the display correlates with the range on the retina. Observers report that appearances of white and black squares are constant and uniform, despite the fact that the retinal stimuli are variable and non-uniform. Human vision uses complex spatial processing to calculate appearance from retinal arrays. Spatial image processing increases apparent contrast with increased white area in the surround. Post-retinal spatial vision counteracts glare.

Keywords — *High dynamic range, intraocular scatter, retinal image.*

DOI # 10.1889/JSID17.11.913

1 Introduction

At times, research on human vision describes detailed information about the stimulus using radiometric, or photometric, measurements of the scene, or test target. Such studies analyzing human image processing need to consider the light distribution of the image falling on the retina after intraocular scatter. High-dynamic-range (HDR) imaging is a good example. HDR images capture and display a greater range of information than conventional images.[1–3] However, scene-dependent scatter in cameras, and in the human eye, controls the ranges of information and appearances.[2–8]

We studied the effects of intraocular scatter and the size of image elements with calculated retinal images. We used the CIE scatter standard[9–11] to calculate the image on the retina. We found large changes in the spatial distribution of light in retinal compared to target images. The retinal luminances changed dramatically with change in the size of target elements in the surround.

2 Design of target

We measured how veiling glare affects tone-scale functions that relate display luminance to appearance in HDR images. To start, we can set aside all the complexities introduced by non-uniformites in target illumination. We will just study patches of light that are uniform in the target.[12] We used a surround that is, on average, equal to the middle of the dynamic range (50% maximum and 50% minimum luminances). Furthermore, these surround elements are made up of different size min and max blocks, spatially unevenly distributed, so that the image has energy over a wide range of spatial frequencies. It avoids the problem that simultaneous contrast depends on the relative size of the white areas and of the test patch.[13] Plots of the radial spatial-frequency distribution *vs.* frequency for these test targets approximate the $1/f$ distribution[14] found in natural images.

We begin with a target made up of film transparencies on a light box. It is a flat, planar display. Our goal is to calculate the changes in that image caused by human veiling glare on the way to the retina. Our "retinal" image is in fact the result of a model that accounts for just one of the many transforms performed by the optics of the eye. The Vos and van den Berg model provides us with a glare spread function that we used to calculate a new planar image than includes the veiling glare found in the human eye. The convolution described below calculates the retinal contrast of each scene pixel. It combines each pixel's luminance with the sum of all scattered light from all other pixels. Our calculation does not include many other properties of the actual retinal image. For example, it does not include the spatial transform caused by the curvature of the retina. It does not calculate the absolute photon count on the retina. Our paper calculates the relative **retinal image contrast** of the original scene as predicted by the CIE Standard Veiling Glare function. The following analysis compares the digital array representing scene contrast with a congruent array of retinal image contrast.

Extended revised version of a paper presented at the Sixteenth Color Imaging Conference (CIC-16) held Nov. 10–15, 2008 in Portland, Oregon.
J. J. McCann is with McCann Imaging, 161 Claflin St., Belmont, CA 02478; telephone/fax 617/484-7865, e-mail: mccann@tiac.net.
A. Rizzi is with the Università degli Studi di Milano, Crème, Italy.

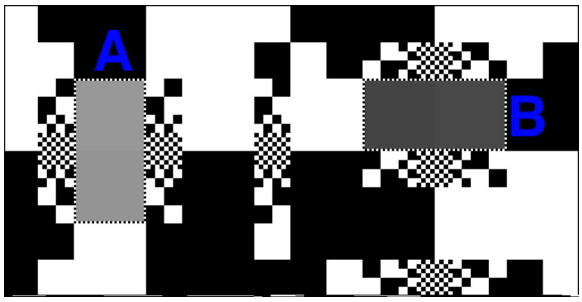

FIGURE 1 — Magnified view of two of twenty sectors that included gray pairs of luminance patches. The left half (sector A) has the same layout as the right (sector B), rotated 90° clockwise. Gray areas in each sector have slightly different luminances. The surrounding areas are identical except for rotation. For each size, there are equal numbers of min and max blocks. The two sectors made up a digital array of pixels 128 high × 256 wide.

2.1 Targets layout

Figures 1 and 2 show the layout of the test targets. Previous papers described magnitudes estimation measurements of the appearances of these targets.[16,17] The display subtended 15.5° × 19.1° (24.6° diagonal). It was divided into 20 square sectors, 3.4° on a side. Each sector contains a pair of adjacent gray squares, with small differences in luminance. The squares are 0.8° on a side, The rest of the square sector contains various sizes of max and min blocks. The two gray square length subtends an angle approximately equal the diameter of the fovea. The smallest min and max blocks (surrounding the gray patches) subtends 1.6 minutes of arc and is clearly visible to observers. The blocks are 2×, 4×, 8×, 16×, 32×, and 64× the smallest block.

We defined the smallest, 1.6-min-arc surround element, to be 1 pixel in our digital array representation of the targets. One sector contained 128 × 128 pixels.

Figure 2 shows a reduced-size illustration of the entire 20 sector target, with four rows of five sectors each. In all the 20 sectors (A through T) are represented by 640 × 512 pixels. In this part of the target, the digital value of minimum black pixels was defined as the measured density of the film images. The entire input array was slightly larger, 750 × 600 pixels. The outer black area was defined to be no light, or opaque. The details follow in the description of the calculation.

TABLE 1 — Luminances and optical densities of the minimum and maximum areas in single- and double-density (contrast) displays.

Target	Max. (cd/m²)	Min. (cd/m²)	Range:1	% Average (cd/m²)	O.D. Min.	O.D. Max.	O.D. Range
Single Contrast	684	1.36	501	50.01%	0.19	2.89	2.70
Double Contrast	441	0.0018	251,189	50.00%	0.38	5.78	5.40

2.2 Single- and double-density targets

Figure 2 shows the 4 × 5-in. film-transparency (single density) test target. The double-density target was the aligned superposition of two identical (single density) films.[15–19]

Two transparencies double the optical densities. [optical density = $\log_{10}$ (1/transmittance)] The whites in each transparency have an optical density (OD) of 0.19; the blacks have an OD of 2.89. The double-density images have a min of 0.38 and a max of 5.78 OD (see Table 1). Both transparency configurations are backlit by four diffused fluorescent bulbs.

Veiling glare for the human visual system (HVS) is a property of the luminance of each image point and the glare spread function (GSF) of the human optical system. Surrounds made up of half-max and half-min luminances have nearly the same glare properties for single- and double-density test targets. The average luminance of the single-density target is 50.10% of the maximum luminance, from a display with a range of ~500:1. The average luminance of the double-density target is 50.00% of its maximum luminance, from a display with a range of ~250,000:1.[15] The effect of glare on the luminances of the gray test areas will be very nearly the same, despite the fact that the dynamic range has changed from 500:1 to 250,000:1. In other words, the black areas (minimum luminances) in both single- and double-density targets are so low, they make only trivial contributions to glare. The white (maximum luminances) in both targets are almost equal and generate virtually all the glare. The layouts of both targets are constant. The physical contributions of glare are very nearly constant. By comparing the calculated retinal contrast with the appearance of these single- and double-density targets, we measured the effects of constant glare on very different dynamic-range displays.[15–19]

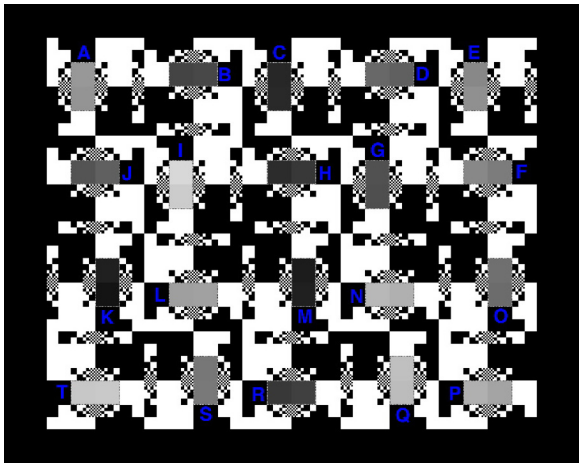

FIGURE 2 — All 20 gray pairs of luminance patches. All gray pairs are close in luminance. The dark-blue letters were used by observers to identify the gray areas. The very low luminance and color were chosen to have minimal effect on luminance.

3 Appearances in single and double density

In order to measure the appearances of the single- and double-density targets, we asked observers to estimate the appearance of each of the 40 test squares. White was assigned to be 100, black was 1. Recent papers describe the observer estimates of appearance for single- and double-density displays with 100, 50, 8, and 0% backgrounds.[13–15] The results show that there is a limited dynamic range that observers can see. The range varies with the amount of white in the background. The range increases with decreased average background whiteness. Observers report the range of appearances from white to black with the target stimuli range of 2.0 $\log_{10}$ units in a 100% white surround. When 50% of the white background is removed, the observers report that blacks are 2.3 $\log_{10}$ units darker than white. With white in only 8% of the background, the white-black range covers 2.7 $\log_{10}$ units. With 100% black background, the range overtakes 4 $\log_{10}$ units. These experiments show that the appearance of a pixel with a fixed luminance value will vary substantially with the amount of white in the background. Furthermore, it shows only minor changes in appearance with very large changes in target dynamic range. Only very dark grays in a black surrounds respond to increased dynamic range.[15–19]

4 Calculated retinal image contrast

This paper compares pairs of digital arrays. The first array represents the high-dynamic range of the targets' scene contrast. The second array is the calculated retinal image contrast.

There are three steps in determining the retinal contrast falling on the retina. First, we need to measure the optical density at each pixel in the target (scene contrast). Second, we need to determine the glare point spread function of human vision. Third, we need to create an efficient algorithm that can read the entire scene array and, taking into account viewing distance and other parameters, transform scene contrast to retinal image contrast.

4.1 Scene contrast

We used a digital editing program to make digital arrays for our targets designs. We sent the high-resolution digital files to a photofinishing lab that used a film recorder to make 4 × 5-in. Ektachrome transparencies, two for each target. We measured the transmission of white, black, and each gray areas using an X-rite 361T densitometer with calibrated standard samples. Since we are concerned with the study of HDR images over a dynamic range of one million to one, we plot our measurements as relative optical density (OD = $\log_{10}$[1/transmittance]). By using these calibration measurements, we made lookup tables (LUTs) to convert target digits to film transmission. We measured the lightbox luminance to be 1056 cd/m^2 with a Minolta 100 C spotmeter. This luminance is associated with optical density OD = 0.

We read the digital array, used to make the targets, and apply the calibration LUT to convert digit to target OD, and then to relative scene luminance. The program reads the 0–255 value in the digital array and replaces it with the floating-point luminance value accurate over 6 log units. This accuracy is assured by the densitometer measurements of each separate single transparency.

4.2 CIE veiling-glare standard

The 1939 CIE meeting reported an empirical description of veiling glare estimated to be proportional to $1/\theta^2$, J. Vos and T. van den Berg collected a series of measurements and wrote a more recent CIE report[9] dated 1999, in which a whole set of formulas are proposed according to the desired degree of precision and other parameters such as the age of the observer and the type of his/her iris pigment.

We decided to report in this paper results from the formula referred to as number eight in the report[9] since it is the most complete. The formula is the following:

$$L_{eq}/E_{gl} = \left[1-0.08\cdot(A/70)^4\right] \cdot\left[\frac{9.2\cdot10^6}{[1+(\theta/0.0046)^2]^{1.5}}+\frac{1.5\cdot10^5}{[1+(\theta/0.045)^2]^{1.5}}\right] +\left[1-1.6\cdot(A/70)^4\right]\cdot\left\{\left[\frac{400}{1+(\theta/0.1)^2}+3\cdot10^{-8}\cdot\theta^2\right]+p \cdot\left[\frac{1300}{\left[1+(\theta/0.1)^2\right]^{1.5}}+\frac{0.8}{\left[1+(\theta/0.045)^2\right]^{0.5}}\right]\right\}+2.5\cdot10^{-3}\cdot p. \quad (1)$$

where θ is the viewing angle from the point from which the light is spread causing the veiling glare, A is the age of the observer, and p is his/her iris pigmentation. This formula measures the equivalent veiling glare in relation to the energy of relative illuminance and is defined as (sr^{-1}). Pigmentation types give the origin of correction parameters that ranges from 0 to 1.21. In the test we used an age of 25 and brown Caucasian pigment.

4.3 Apply glare spread function

We wrote a program to compute the glare spread function (GSF) from the CIE formula [our Eq. (1)] to convolve it with the input target image in order to convert it into retinal image-contrast values.[18] Figure 3 plots the log of the amount of veiling glare *vs.* log visual angle between the central point of light and the position of eccentric retina receiving the glare. To avoid computational problems near the edges of the target, we pad the target image array with null values (luminance = 0). (This reflects quite well the conditions of the experiment that has been held in a dark room in which the target was the only light source and everything was painted dark in order to avoid reflections.) We made a

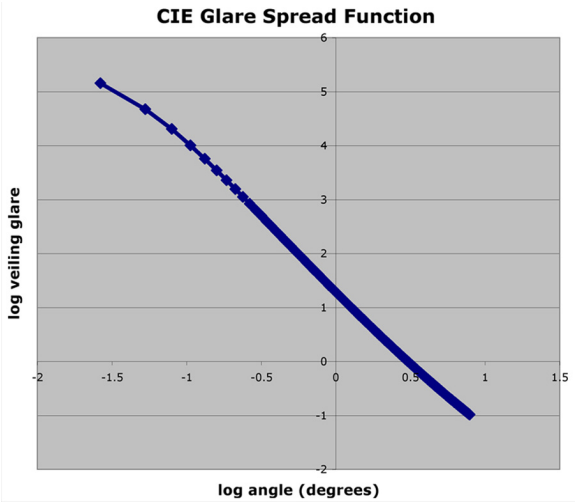

FIGURE 3 — Glare spread-function filter plotted on log scales.

square filter twice the size of the longer target side. This filter calculates the distance-dependent scatter contribution from all other pixels using our Eq. (1). We transformed the filter into the spatial-frequency domain and calculated the glare for each pixel with the fft convolution. Each target pixel is the sum of that pixel's luminance, plus the amount of light scattered into that pixel from all other pixels in the target, minus the light scattered out of that pixel. The CIE standard for veiling glare covers angles from 1/100° to 100°. The dynamic range of veiling glare (vertical axis) in the equation covers 1,000,000 to 1/1000 units of ratio of equivalent luminance in cd/m^2/glare illuminance at the eye in lux.

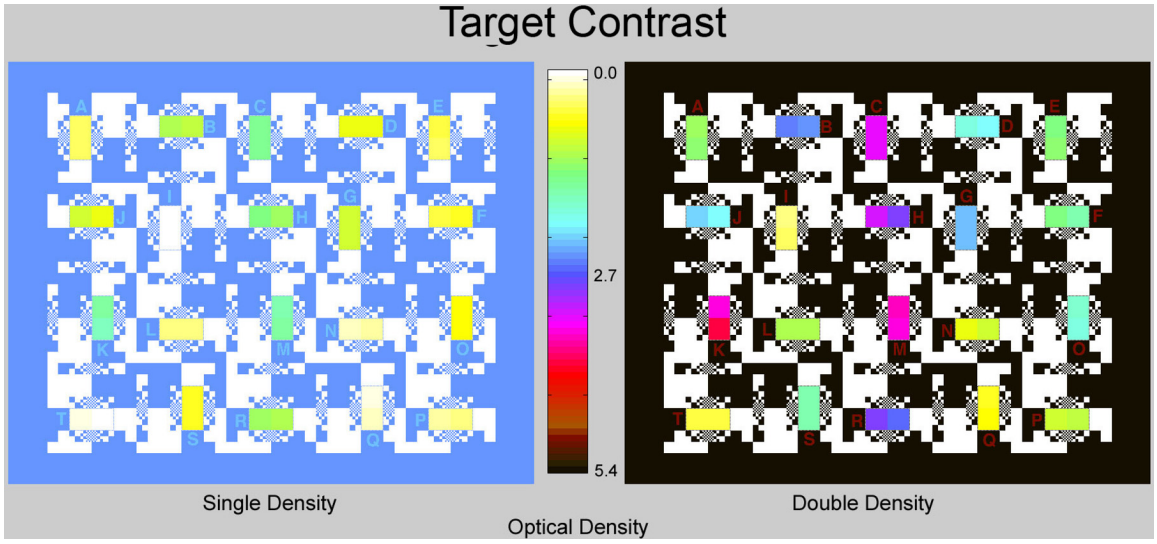

FIGURE 4 — A pseudocolor rendering of target luminance. The double-density target has a range of 5.4 (OD); the single density has a 2.7 (OD) range. The colorbar in the center identifies the color of each optical density over the range of 5.4 log units. The single- and double-density targets are very different stimuli.

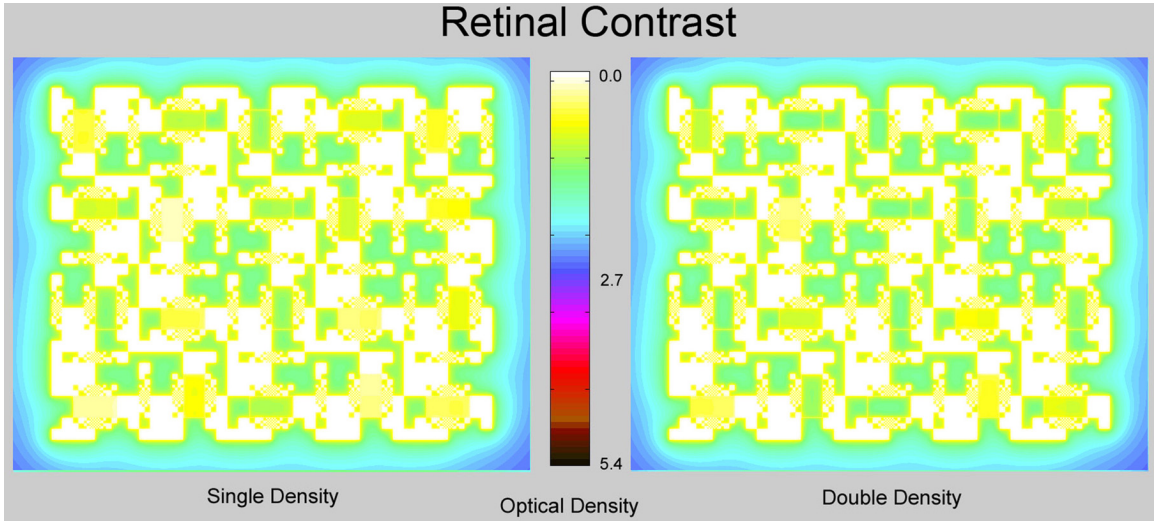

FIGURE 5 — Figure 5 renders the retinal image contrast using the same pseudocolor used above in Fig. 4. Both the single- and double-density retinal ranges are roughly 2.0 (OD). The single- and double-density images are very similar retinal stimuli.

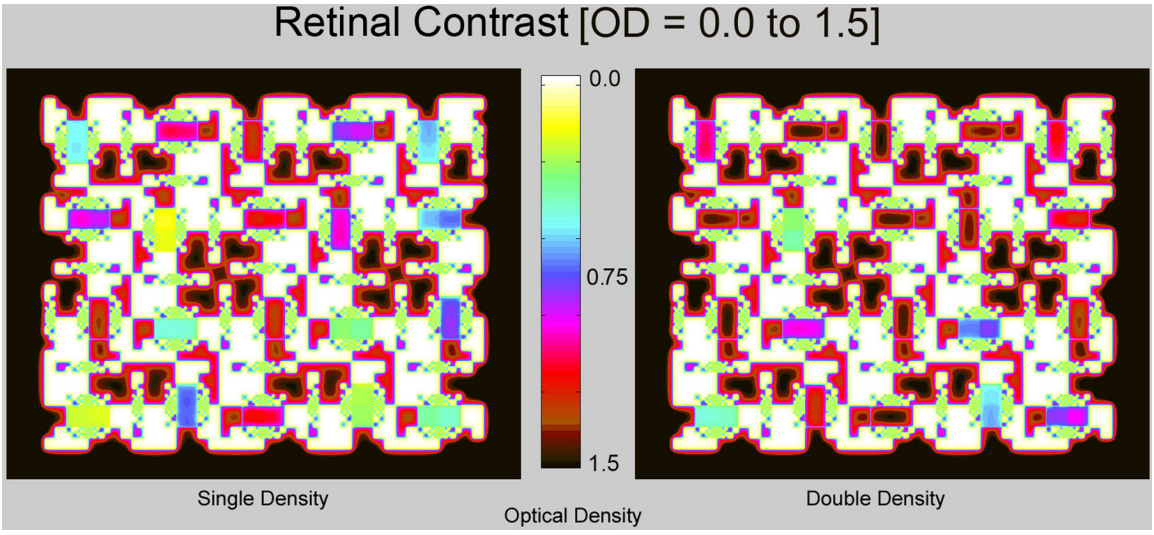

FIGURE 6 — A different rendition of the range of retinal image contrast than shown in Fig. 5. To improve pseudocolor discrimination, the range of the colormap in this plot is only 1.5 (OD). This colormap rendering brings out the more subtle differences between single- and double-density retinal images.

5 Analysis: Scene contrast *vs.* retinal contrast

The range of target luminances for the single-density target was 2.7 OD units. It is not possible to reproduce this range on print and conventional displays. The double-density target made the problem much more severe. We use a 64-pseudocolor colormap to render the target luminance range of 5.4 OD units. The maximum luminance was white and the minimum was black. The colors, in decreasing luminance, are white, yellow, green cyan, blue, magenta, red brown, and black. Rendering the range of 5.4 OD target luminances in 64 steps gives a range of 0.084 OD per individual colorbar element. We show the pseudocolor scale in the center of Figs. 4–6. The color-map images illustrate the substantially different ranges of luminance measured in the 2.7 OD single-density and 5.4 double-density targets.

We used the same color map to render the calculated retinal contrast of the single-density and double-density images (Fig. 5). Unlike the Fig. 4 renditions, the retinal image contrasts are very similar to each other. Intraocular scatter reduces the 5.4-OD dynamic range of the double-density target to about 2.0 log units on the retina. It is only slightly darker than the single-density retinal contrast array.

The calculated retinal contrasts show that intraocular glare limits the range of the image to roughly 2.0 OD units for these 50% white targets. The white surround patches have nearly the same densities in both target and retinal contrasts. The black surround squares have very different densities in the targets, but because of scatter, they are nearly the same in the range on the retina. The 40 gray test patches have twice the density in the double-density target. That means that more squares have optical densities greater than 2.0. In other words, more than half the squares are below the limit determined by scattered light. Hence, the gray test squares in the double-density targets show more retinal similarity. Recall that the observer data from discrimination experiments was limited to the 2.3 OD range.[17]

Figure 6 shows a different colorbar rendering of retinal image contrast from that in Figs. 4 and 5. Here, we spread the same 64-colorbar elements over only 1.5 OD,

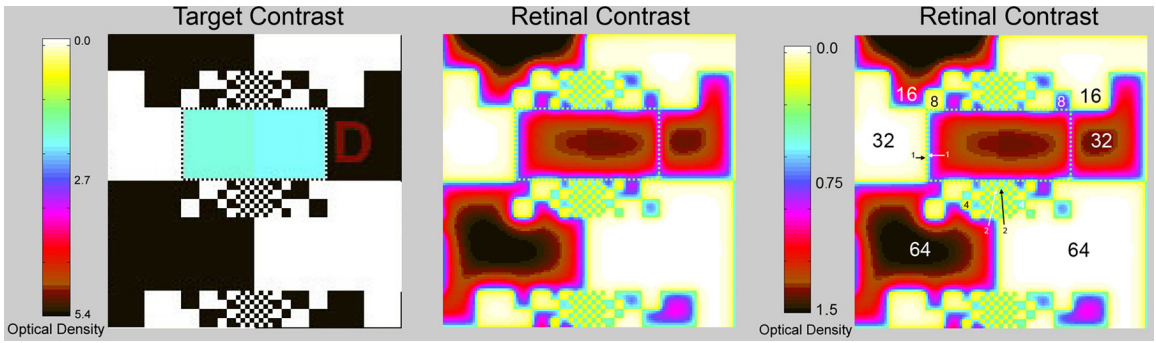

FIGURE 7 — The target contrast (left) (colormap range = 5.4) (center) the retinal image contrast, and (right) the annotated retinal contrast using the same pseudocolor map rendition in Fig. 6 (colormap range = 1.5). The annotation numbers 64, 32, ..., 1 show the relative sizes of sides of the white and black squares. It shows only double-density area D and its surround. It illustrates the effect of intraocular scatter on different size white and black squares.

instead of 5.4 OD. Rendering the range of 1.5-OD target contrast in 64 steps gives a range of 0.0234 OD per individual colorbar element. This rendition shows the after-scatter values of the 20 pairs different gray patches in the targets. In the single-density target, we see a range of different colors for the different transmissions. In the double-density target, we see that intraocular scatter made many of the darker-gray squares more similar.

6 Discussion

Veiling glare from a single pixel decreases with distance away from that pixel. Figure 3 shows the falloff of scattered luminance *vs.* distance. This value at large distances is very small, but a small contribution comes from every pixel in the image. The sum of many very small contributions is a significant number. The greater the % white in the scene, the more the glare, the lower the contrast of the retinal image.

The background in these images has a range of different sizes of uniform white or black squares. Each white pixel scatters a fraction of its light into surrounding pixels. In turn, each pixel receives a distance-dependent fraction of light from all other pixels. A pixel in the center of a large white square has the highest retinal luminance because there are many surrounding white pixels that contribute a larger fraction of their scattered light. Similarly, the lowest luminance pixels are found in the center of the largest black square since it is the furthest from white-pixel scatter sources. The highest ratio of retinal radiances (retinal contrast) is the ratio of the center pixels in largest white/black squares. The same logic shows that the smallest white/black retinal contrast is the ratio of the smallest, single-pixel retinal luminances. The results of the calculated retinal image show retinal luminance ratios from as high as 17.46 to 1 to as low as 2.11 to 1 (see Fig. 7 and Table 2).

Another feature of retinal images is the conversion of uniform target luminance to gradients of retinal luminance. The target was designed to have uniform patches of white and black squares. At each white/black edge, intraocular scatter transforms the sharp edge into a much smoother transition with gradients. The slope of that gradient varies with the neighboring pixels. The simple uniform target luminances have been transformed into a very complex array of gradients. Figure 7 (left) shows the array of target luminances using colorbar = 5.4. Figure 7 (center and right) shows the array of retinal contrasts using colorbar = 1.5. The retinal image is made of many complex gradients. The two different gray squares are very close in retinal luminance; in fact, they are almost indistinguishable in the pseudocolor rendering. Observer magnitude estimates of Area D were 11.9 ± 2.0 (left) and 6.9 ± 3.1 (right), on a scale of white = 100 and black =1.[16] Observers are able to discriminate small differences in retinal luminance. All white surround squares have identical target luminances, as do all black surround squares. However, both white and black squares have variable retinal luminances depending on the size of the square, as well as position in the surround. Constant target luminance does not ensure constant retinal luminance.

The retinal contrast image also shows that the largest squares (lowest spatial-frequency components) have the largest retinal luminance ratios. Nevertheless, the squares look the same whites and blacks. Regardless of the retinal luminances, the spatial processing mechanisms make the appearances the same. This suggests that different spatial-frequency channels have different appearance outputs for constant retinal luminance inputs. Table 2 lists the target and retinal luminances for variable size white and black surround squares in Fig. 7. The locations of the squares listed are shown in Fig. 7 (right). The selection of these squares is arbitrary and does not represent any statistical analysis.

Table 2 shows the relative optical densities of retinal contrasts for different sized white/black pairs. It shows the colorbar rendering of these retinal calculations. It lists the difference in OD and the ratio of retinal luminances at the centers of the square.

The final topic is the appearance of the white/black surround patches. Do they appear to have variable appearance as implied by their retinal contrast? Do they appear the same white and black for all sizes of squares? Although not measured experimentally with multiple observers and multiple trials, we observed that the white/black contrast appears the same regardless of the size of the white/black squares. Intraocular scatter controls the range of retinal luminance, which in turn controls the range of usable display dynamic range. The rate of change of white/black appearance scales varies with the amount of white in the surround.[15–19] The

TABLE 2 — Data and colormap rendering of white and black squares shown in Fig. 7. The first column lists the areas sampled (Fig. 7 – right). The second (white) and fourth (black) columns list retinal contrast (OD). The third and fifth column show the colormap values for these densities. The sixth column lists the difference in OD. The last column lists the ratios of luminances from the center of the white and black squares. The second row shows the input target luminances for all squares. The remaining rows show typical output samples for retinal luminance in different size squares. The third through ninth rows show sample values for the largest square (64×) through the smallest square (1×). Retinal contrast values vary considerably with the surrounding portion of the image. These are typical values identified in Fig. 7. The size of white and black squares has considerable influence on the retinal luminance, contrast, and white/black (*W/B*) ratios.

	DD white OD		DD black OD		W/B contrast OD	W/B edge ratio
Target	0.00		5.4		5.40	251,188.64
DD 64x	0.08		1.02		1.24	17.46
DD 32x	0.09		0.89		1.08	12.02
DD 16x	0.17		0.61		0.86	7.31
DD 8x	0.24		0.43		0.59	3.93
DD 4x	0.25		0.51		0.32	2.11
DD 2x	0.35		0.47		0.22	1.64
DD 1x	0.46		0.53		0.16	1.45

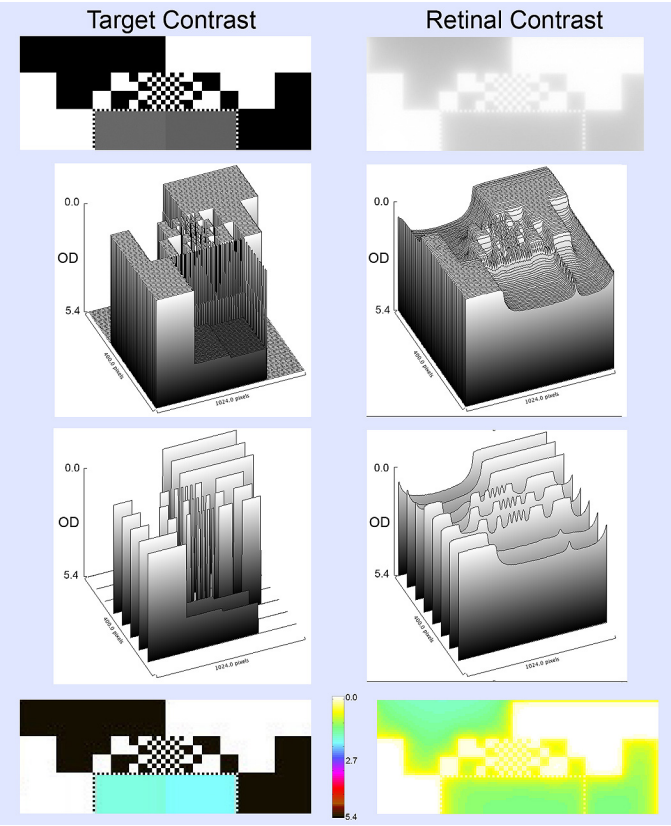

FIGURE 8 — Comparison of the target contrast (left) with retinal contrast (right), for a portion of the image in section D. These comparisons use the same scale (5.4 OD) for the left and right columns. The top row compares target and retinal contrasts. The second pair of comparisons shows 100 horizontal plots of contrast. The next row of surface plots shows eight contrast slices. The bottom pair is the pseudocolor map used in Figs. 4 and 5. All plots show that the uniform high-dynamic-range (OD = 5.4) target is transformed by glare into a non-uniform low-dynamic-range retinal image. Of particular interest are size-dependent effects on white/black edges. While all whites have the same target luminances, their retinal values vary considerably with the size of the white area. The retinal values of the black squares vary with both size and position in the image. Each sharp white/black edge in the target is transformed into image-dependent gradients in retinal contrast.

mechanism responsible for simultaneous contrast makes smaller retinal-luminance ratios appear more different. We have the paradox that lower retinal contrast generates higher apparent contrast. The data shown here is important in evaluating the design parameters of display devices. First, the limits of usable dynamic range of a display depends on the displayed image. Second, appearances of whites and black are spatial frequency dependent.

The study of the white/black edges in the variable square surrounds suggests that apparent contrast mechanisms vary with spatial-frequency channels. The calculated retinal image shows that smallest squares (highest spatial-frequency components) have the smallest retinal luminance ratios. Figure 8 illustrates the significant effects of intraocular scatter on the retinal image. It shows one of 20 different pairs of gray squares and its surround in the double-density target. The gray squares sections have different transmissions near 2.7 OD. All sizes of white squares have OD 0.0 and all blacks had 5.4 OD.

Figure 8 uses four different visualizations to compare target and retinal images: scaled contrast, eight horizontal contrast plots, surface plots of contrast, and pseudocolor. Intraocular scatter transforms high-dynamic-range, uniform, constant square targets (left) into low-dynamic-range, gradients with variable retinal contrast (right).

Human spatial image processing transforms this complex retinal image so that all "target whites" appear as the same white and all "target blacks" appear as the same black. HDR image-processing techniques that attempt to mimic human vision need to differentiate the *optical* effects of intraocular glare from the *neural* spatial-image processing. Both optical and neural mechanisms show significant scene-dependent alteration of the image. These different image-dependent processes tend to cancel each other, making their presence less obvious.[17–19]

7 Conclusions

We measured the target luminance at each pixel, and calculated the retinal contrast array using the CIE Standard glare spread function. Intraocular glare reduced the HDR target luminances to much smaller ranges, depending on image content. These limited-range retinal images are consistent with data from observer discrimination experiments. Furthermore, the calculations show that there is no simple relationship between the retinal contrast of a pixel and its appearance between white and black. Observers report that the appearances of white and black squares are constant and uniform, despite the fact that the retinal stimuli are variable and non-uniform. Human vision uses complex spatial image processing to calculate appearance from retinal contrast arrays.

Acknowledgments

We want to thank Ivar Farup for his collaboration on the program, and Tom van den Berg with Joris Coppens for their discussions of the glare spread function, Marzia Pezzetti for experimentation and Mary McCann for helpful discussions. This work has been supported by the PRIN-COFIN 2007E7PHM3-003 project by Ministero dell'Universitá e della Ricerca, Italy.

References

1 E. Reinhard *et al.*, *High Dynamic Range Imaging Acquisition, Display and Image-Based Lighting* (Elsevier, Morgan Kaufmann, Amsterdam, 2006), Chap 6.
2 J. J. McCann, "Art science and appearance in HDR images," *J. Soc. Info. Display* **15**(9), 709–719 (2007).
3 J. J. McCann and A. Rizzi, "Camera and visual veiling glare in HDR images," *J. Soc. Info. Display* **15**(9), 721–730 (2007).
4 J. J. McCann and A. Rizzi, "Optical veiling glare limitations to in-camera scene radiance measurements," *ECVP 2006 Abstracts, Perception* **35**, Supplement, 51 (2006).
5 J. J. McCann and A. Rizzi, "Spatial comparisons: The antidote to veiling glare limitations in HDR images," *Proc. ADEAC/SID&VESA*, 155–158 (2006).

6 J. J. McCann and A. Rizzi, "Limits of HDR images: Image capture and image display," *Proc. IS&T/SID Color Imaging Conference, Late Breaking News section* (2006).
7 J. J. McCann and A. Rizzi, "Veiling glare: The dynamic range limit of HDR images," *Human Vision and Electronic Imaging XII*, eds. B. Rogowitz, T. Pappas, and S. Daly, *Proc. SPIE*, 6492-41 (2007).
8 J. J. McCann and A. Rizzi, "Spatial comparisons: The antidote to veiling glare limitations in image capture and display," *Proc. IMQA 2007*, Chiba, E-1 (2007).
9 J. J. Vos and T. J. T. P. van den Berg, "CIE Research Note 135/1, Disability Glare," ISBN 3 900 734 97 6 (1999).
10 CIE, "146 CIE equations for disability glare," in 146/147: CIE Collection on Glare (2002).
11 T. J. T. P. van den Berg, "Analysis of intraocular straylight, especially in relation to age," *Optometry and Vision Science* **72**, No 2, 52–59 (1995).
12 J. J. McCann, "Aperture and object mode appearances in images," in *Human Vision and Electronic Imaging XII*, eds. B. Rogowitz, T. Pappas, and S. Daly, *Proc. SPIE*, 6292-26 (2007).
13 J. J. McCann and A. Rizzi, "The spatial properties of contrast," *Proc. IS&T/SID Color Imaging Conference*, 51–58 (2003).
14 D. J Tolhurst *et al.*, "Amplitude spectra of natural images," *Ophthalm Physiol. Opt.* **12**, 229–232 (1992).
15 A. Rizzi *et al.*, "Measuring the visible range of high dynamic range images," *ECVP07, European Conference on Visual Perception*, Arezzo, **36** ECVP Abstract Supplement (2007).
16 A. Rizzi *et al.*, "Glare-limited appearances in HDR images," *Proc. Color Imaging Conference* (2007).
17 A. Rizzi and J. J. McCann," Glare-limited appearances in HDR images," *J. Soc. Info. Display* **17**, No. 3 (2009).
18 A. Rizzi *et al.*, "Separating the effects of glare from simultaneous contrast," paper *Proc. SPIE/IS&T Electronic Imaging Meeting* (2008).
19 J. J. McCann and A. Rizzi, "Appearance of high-dynamic range images in a uniform lightness space," *Proc. CGIV 08/IS&T, 4th European Conference on Colour in Graphics* (2008).

John McCann (1964 AB. degree, Biology, Harvard) worked in and managed the Vision Research Laboratory, Polaroid (1961–1996). His 120 publications have studied Retinex theory, rod/Lcone color interactions at low light levels, appearance with scattered light, and HDR imaging. He is a Fellow IS&T, OSA; past-President IS&T, Artists Foundation, Boston. He continues his research on color vision. He received the SID Certificate of Commendation, IS&T/OSA 2002 Edwin H. Land Medal, and IS&T Honorary Member.

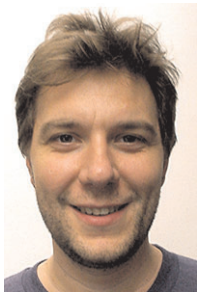

Alessandro Rizzi received his degree in computer science from the University of Milano and his Ph.D. in information engineering from the University of Brescia. He is currently an assistant professor and senior research fellow at the Department of Information Technologies at the University of Milano. Since 1990, he has been performing research in the field of digital imaging and vision. His main research topic is color information with particular attention to color-perception mechanisms. He is the coordinator of the Italian Color Group.